Physics – Uspekhi **47** (9) 907 – 922 (2004)

REVIEWS OF TOPICAL PROBLEMS

PACS numbers: **43.25.+y**, 47.40.Nm, 87.54.Hk

Self-action effects for wave beams containing shock fronts

O V Rudenko, O A Sapozhnikov

DOI: 10.1070/PU2004v047n09ABEH001865

Contents

Abstract. **The review covers experimental and theoretical studies of the self-action effects observed for intense wave beams with sawtooth time profiles. For sawtooth waves in quadratic nonlinear media, inertial self-focusing and defocusing processes caused by the formation of acoustic streaming and heating due to nonlinear energy dissipation at shock fronts are discussed. Self-refraction of shock-wave pulses is considered, which leads, in particular, to the saturation of the maximal field achieved by focusing. For cubic nonlinear media, where a sawtooth wave contains both compression and rarefaction shocks, the self-focusing process is studied in the presence of its strong competition with nonlinear damping. New mathematical models, their symmetry properties and exact solutions, and the results of numerical simulation are described. A general picture of the state of the art in this field is given.**

1. Introduction

The term *self-action* in wave physics is mainly used for the description of nonlinear effects in which an intense wave acquires an amplitude-dependent absorption coefficient or propagation velocity without changing its profile. In the first case, one speaks of a nonlinear wave absorption (or amplification) and in the second case of a nonlinear dispersion. We note that precisely because the wave profile is constant (or slowly varying), the wave can be considered as a single object with a certain propagation velocity. Self-action effects started to arouse considerable interest after the discovery of the self-focusing of light. The history of this problem is described in detail in Refs [1, 2]. The steady-state excitations in nonlinear optics are quasi-harmonic waves. They are stable because of the strong dispersion that prevents generation of waves at other frequencies, that is, that prevents the distortion of the initial wave profile. Self-action of waves is related to the response of the medium at the fundamental frequency; this response appears due to the cubic nonlinearity and higher-order odd nonlinearities of the medium. However, for coupled waves of different frequencies, self-action can also occur in a quadratic nonlinear medium [3].

Some basic results of the light self-focusing theory are important not only for the physics of strong laser radiation but also for the general theory of nonlinear waves [4]. The first theoretical works on self-focusing (see Refs [5 – 7]) had a considerable impact on the development of similar studies in other fields of physics, in particular, in nonlinear acoustics and the general theory of nonlinear wave beams propagating in weakly dispersive media.

We note that in recent works, the term 'self-focusing' is widely used in a totally different meaning (see, e.g., Refs [8 – 12]). The second meaning implies time inversion of the signal for its focusing into an inhomogeneous medium, and it emerged after the development of adaptive sound and ultrasound sources based on this technique. An established term brought into use in a new meaning can cause much misunderstanding.

Harmonic waves are not the only example of steady-state excitations propagating in a nonlinear medium. Moreover, in a nondispersive or weakly dispersive medium, finite-amplitude waves that are initially harmonic become unstable in the course of propagation, their profile becomes distorted, and the spectrum is quite rapidly spread due to the generation of higher harmonics. In a medium with certain types of nonlinearity and dispersion, solitons can become steady-state signals. A medium with weak dispersion allows a new possibility for the propagation of steady signals with a broad frequency spectrum. The dispersion is considered weak if the typical dephasing distance for interacting waves of different frequencies (the coherence length) is much larger than the nonlinear interaction length. In the opposite case, one speaks of 'strong dispersion'. It is known that an intense wave

O V Rudenko, O A Sapozhnikov Physics Department, M V Lomonosov Moscow State University, Vorob'evy Gory, 119992 Moscow, Russian Federation
Tel./Fax (7-095) 939 29 36, (7-095) 939 29 52
E-mail: rudenko@acs366.phys.msu.ru, oleg@acs366.phys.msu.ru

Received 18 March 2004, revised 25 April 2004
Uspekhi Fizicheskikh Nauk **174** (9) 973 – 989 (2004)
Translated by M V Chekhova; edited by A M Semikhatov

propagating in a medium with weak dispersion is distorted, the distortion increasing with the propagation distance. Eventually, this distortion leads to the smoothing of small details and to the formation of profiles with a universal shape [13]. For instance, a single pulse initially localized in time acquires the shape of an N-wave due to the joint action of the quadratic nonlinearity, absorption, and diffraction. Such waves are formed in explosions [14] and in the motion of supersonic jets [15]. A periodic plane wave takes a 'sawtooth' shape, which is a sequence of straight sections of equal slope connected by shock fronts. Figure 1 presents a profile of such a sawtooth wave recorded at the exit from the near-field zone of a spherical piezoelectric ultrasonic source [16]. The ultrasonic wave, initially harmonic, was much distorted during its propagation and finally became sawtooth-like. Measurements at growing distances show that the profile is practically independent of the distance and the only changing parameter is the amplitude of the wave. Sawtooth acoustic waves in liquids were first observed in the 1950s and were explained by the effect of the quadratic nonlinearity of the medium [17]. In media with more complicated properties, other types of asymptotically universal profiles can be formed. For instance, in the presence of relaxation, the wave profile behind the shock front is not straight but has a complicated shape depending on the relaxation parameters. Figure 2 shows the profile of an intense acoustic pulse after its propagation through a liquid in the presence of relaxation (acetic acid) [18]. In contrast to the wave profile in Fig. 1, here the shock front is followed by a smooth rise. The shape of the pulse is determined by the parameters of the relaxation process. Competition between nonlinear and dissipative processes makes the profiles of such waves quasistable. Propagation does not change their shapes; the only parameters that vary are their peak amplitudes; in the case of separate pulses, the time duration can vary as well.

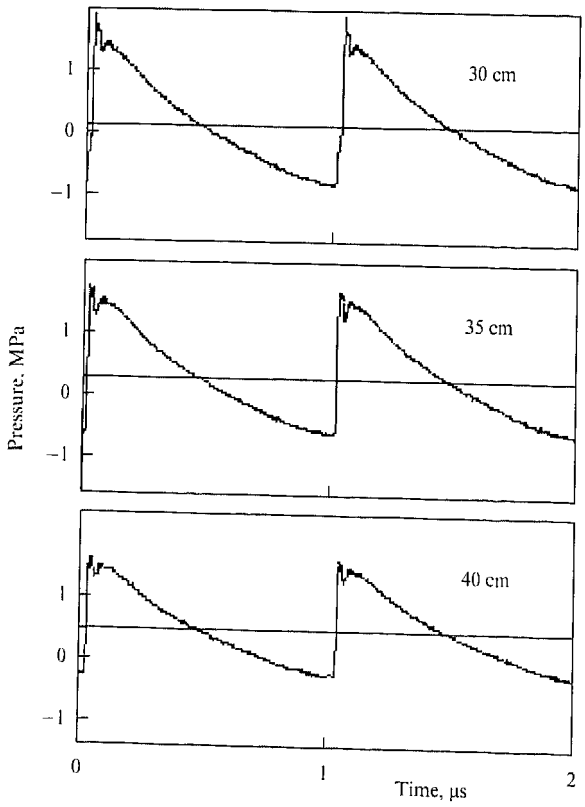

Figure 1. The profile of an intense ultrasonic wave with the frequency 1 MHz generated by a piezoelectric source and measured at various distances from the near-field zone.

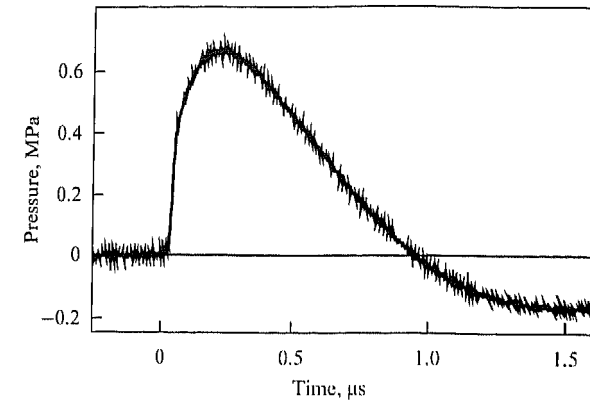

Figure 2. The profile of an acoustic pulse with a shock front propagating through a liquid with relaxation.

As we have already mentioned, a quasi-harmonic wave in a dispersive medium has a similar quasistability property. For this reason, the self-action of such a wave can be described by passing from field equations involving spatial variables and time to simpler models like the nonlinear Schrödinger equation for a variable (the complex amplitude) that depends only on spatial coordinates. This method of eliminating the time dependence can sometimes help to simplify nonlinear equations describing the behavior of wave beams with shocks.

The present work is focused on the effects of spatial self-action for waves with broad frequency spectra whose profiles contain breaks or steep shocks of a finite width that is small compared to the wave period or to the typical pulse duration.

2. Self-action of sawtooth ultrasonic wave beams due to the heating of the medium and the formation of acoustic streaming

The fact that acoustic beams can manifest thermal self-action similarly to laser beams was pointed out in Ref. [19]. In a medium where the sound velocity c grows with increasing temperature [an example is water at room temperature, for which $\delta = (\partial c/\partial T)_p/c > 0$], an acoustic beam is defocused, while in a medium with a negative temperature coefficient $\delta < 0$ (the majority of liquids), self-focusing of the acoustic beams occurs. A review of the first theoretical works can be found in Ref. [20]. Later, this effect was observed in experiment [21, 22]. References to further publications can be found in reviews [23, 24] and in monograph [25]. However, this list is not complete because the self-action of harmonic acoustic waves is still under study [26]. Considerable attention is drawn to the thermal self-action of quasi-harmonic acoustic waves because many interesting results obtained in nonlinear optics have their counterparts in this field of acoustics [27].

Thermal self-action is caused by the variation of the average temperature of the medium due to the absorption of the wave energy; the corresponding nonlinear mechanism is nonlocal (the scale of thermal inhomogeneities is much larger than the wavelength) and slow (formation of a thermal lens takes much longer than one period of the wave). Similar inertial self-action can occur through the formation of hydrodynamic streams in the medium ('acoustic streaming')

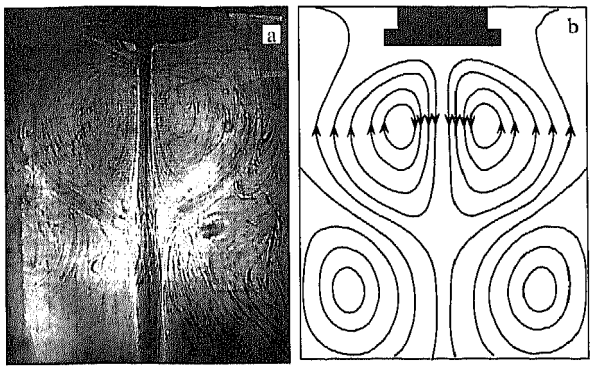

Figure 3. (a) Shadow picture of inhomogeneities induced by a vertical ultrasonic beam with the frequency 1 MHz in glycerin. Illumination was performed by pulsed laser radiation. The ultrasound source is at the top. Darker regions correspond to higher temperatures. Fine periodic horizontal lines in the central part are inhomogeneities induced by the ultrasonic wave. (b) The observed structure of thermodynamic streams corresponding to the shadow picture on the left. The source is shown in black and the acoustic beam in gray.

due to the radiation pressure of an intense shock wave [20]. This mechanism always leads to defocusing because the drift caused by streaming makes the wave velocity increase in the central part of the beam, where the ultrasound intensity is higher and hence streaming is stronger.

We note that the inertial self-action effects described above are rather simple and have no pronounced nonlinear features. Because both the heating of the medium and the formation of acoustic streaming take place over the course of many seconds or even minutes, the above self-action effects are similar to the acoustic modulation by external heat sources or externally induced streams acting on the beams as thermal or convection lenses. These processes seem to have been observed many times in the 1950s, after the development of piezoelectric transducers for the generation of strong ultrasound in liquids [28] (V A Burov and L K Zarembo, private communications), but they were not interpreted as nonlinear effects. The structure of hydrodynamic streams can become more complicated in the presence of gravitational thermoconvection caused by the heating of the medium due to the wave dissipation. For instance, an interesting 'wineglass' configuration of streams — a vertical acoustic beam in glycerin forming two opposite axially symmetric toroidal vortices — was observed in Ref. [29]. The inner vortex was caused by an acoustic stream and the outer was formed due to thermoconvection (Fig. 3). In the region where the vortices almost compensated each other and the resulting velocity was small, the sound intensity was an order of magnitude higher and the beam was two or three times narrower.

A simplified system of equations describing thermal self-action was derived in Ref. [30] in the case corresponding to the experiment in Ref. [29], i.e., with both acoustic and thermoconvection streams taken into account. For an axially symmetric problem, the equations are given by

$$\frac{\partial}{\partial\tau}\left[\frac{\partial p}{\partial x}-\frac{1}{c}\left(\frac{U_x}{c}+\delta T\right)\frac{\partial p}{\partial\tau}-\frac{\varepsilon}{c^3\rho}\,p\,\frac{\partial p}{\partial\tau}-\frac{b}{2c^3\rho}\,\frac{\partial^2 p}{\partial\tau^2}\right]=\frac{c}{2}\,\Delta_\perp p\,, \tag{1}$$

$$\frac{\partial U_x}{\partial t}+U_x\,\frac{\partial U_x}{\partial x}+U_r\,\frac{\partial U_x}{\partial r}=-\frac{1}{\rho}\,\frac{\partial P_0}{\partial x}+\frac{\eta}{\rho}\,\Delta_\perp U_x+F-\beta g T\,, \tag{2}$$

$$\frac{\partial}{\partial x}(rU_x)+\frac{\partial}{\partial r}(rU_r)=0\,, \tag{3}$$

$$\frac{\partial T}{\partial t}+U_x\,\frac{\partial T}{\partial x}+U_r\,\frac{\partial T}{\partial r}=\frac{\varkappa}{\rho c_p}\,\Delta_\perp T+\frac{c}{c_p}\,F\,. \tag{4}$$

Here, x and r are cylindrical coordinates, the x axis coincides with the axis of the beam, $\tau = t - x/c$ is the 'retarding time' in the reference frame moving with the speed of sound c together with the wave, p is the acoustic pressure, $\mathbf{U} = (U_x, U_r)$ is the velocity of the hydrodynamic flow, T is the temperature of the medium, $\Delta_\perp$ is the Laplacian with respect to the radial coordinate, ε and b are the nonlinearity and dissipation parameters [31], η is the shear viscosity, β is the thermal coefficient of volume expansion, c_p and $\varkappa$ are the heat capacity and heat conductivity of the medium, and g is the acceleration of gravity. Equation (1) describes the beam with the acoustic nonlinearity, dissipation effects, and diffraction taken into account; in contrast to the well-known Khokhlov–Zabolotskaya–Kuznetsov equation [32], Eqn (1) additionally describes modulation of the wave velocity due to the variation of the temperature T and the longitudinal flow velocity U_x. Absorption of the wave leads to the generation of streams in an incompressible liquid, which is described by Eqns (2) and (3), as well as to changes in the temperature field, whose dynamics are described by Eqn (4). In a quasi-Eckart stream [31], the pressure P_0 depends on x, t and does not depend on r. The radiation force on the right-hand sides of (2) and (4) is

$$F=\frac{b}{c^5\rho^3}\left\langle\left(\frac{\partial p}{\partial\tau}\right)^2\right\rangle, \tag{5}$$

where the angular brackets denote averaging over fast acoustic oscillations (over time τ).

The system of coupled nonlinear equations (1)–(4) allows us to describe both harmonic waves and strongly distorted waves with a broad frequency spectrum. In the case where the acoustic nonlinearity is not essential, which formally means that $\varepsilon = 0$, the 'fast time' in Eqn (1) can be eliminated by putting

$$p = A(x, r)\exp(-\mathrm{i}\omega\tau)\,. \tag{6}$$

For the complex amplitude A, we then obtain the parabolic equation

$$\frac{\partial A}{\partial x}+\mathrm{i}k\left(\frac{U_x}{c}+\delta T\right)A+\frac{b\omega^2}{2c^3\rho}\,A=\frac{\mathrm{i}}{2k}\,\Delta_\perp A\,. \tag{7}$$

The remaining equations (2)–(4) are related to Eqn (7) through 'force' (5), which now takes the form

$$F=\frac{b\omega^2}{c^5\rho^3}\,A^2\,. \tag{8}$$

In those cases where the acoustic nonlinearity is important, the 'fast time' can be eliminated only in the geometric acoustics approximation. Assuming

$$p=p\left(x,r,\theta=\tau-\frac{\psi(x,r)}{c}\right) \tag{9}$$

in Eqn (1), we obtain

$$\frac{\partial p}{\partial x}-\frac{\varepsilon}{c^3\rho}\,p\,\frac{\partial p}{\partial\theta}-\frac{b}{2c^3\rho}\,\frac{\partial^2 p}{\partial\theta^2}+\frac{\partial p}{\partial r}\,\frac{\partial\psi}{\partial r}+\frac{p}{2}\,\Delta_\perp\psi=0\,, \tag{10}$$

$$\frac{\partial\psi}{\partial x}+\frac{1}{2}\left(\frac{\partial\psi}{\partial r}\right)^2+\frac{U_x}{c}+\delta T=0 \tag{11}$$

for a wavelength that is small compared to the size of thermal and hydrodynamic inhomogeneities. Transport equation (10) resembles the Burgers equation for plane nonlinear waves [31], but differs from it by the last two terms, which take variations in the sizes of ray tubes into account. Equation (11) is the eikonal equation describing the bending of beams due to the temperature and hydrodynamic field inhomogeneities.

Equation (10) describes the formation and subsequent propagation of a sawtooth wave whose shock front has a finite width. Each period of the wave profile is described by the formula [31]

$$p(x,r,\theta) = A(x,r)\left[-\frac{\omega\theta}{\pi} + \tanh\left(\frac{\varepsilon}{b}A(x,r)\theta\right)\right], \quad -\frac{\pi}{\omega} \leqslant \theta < \frac{\pi}{\omega}. \tag{12}$$

Expression (12) can be considered a generalization of (6) to the case of an acoustically nonlinear problem. The unknown function A giving the 'peak' pressure in the 'saw' is analogous to the harmonic wave amplitude in (6).

Substituting (12) in Eqns (10) and (5), we obtain the two equations

$$\frac{\partial A}{\partial x} + \frac{\varepsilon\omega}{\pi c^3\rho}A^2 + \frac{\partial A}{\partial r}\frac{\partial\psi}{\partial r} + \frac{A}{2}\Delta_\perp\psi = 0, \tag{13}$$

$$F = \frac{2}{3\pi}\frac{\varepsilon\omega}{c^5\rho^3}A^3. \tag{14}$$

In Eqn (13), the term proportional to εA^2 describes nonlinear absorption, which grows as A increases. In contrast to (8), the 'force' (14) is determined not by the dissipation parameter b but only by the nonlinearity ε. Therefore, sawtooth waves should also manifest self-action effects in ideal media, where the usual absorption is absent. We also note that Eqn (14) gives the dependence $F \sim A^3$ but not $F \sim A^2$, as in harmonic waves [see Eqn (8)]. This means that passing from the regime of harmonic waves to the nonlinear regime with sawtooth profiles leads to a considerable increase in both the radiation force and the heat generation rate in the medium under the influence of an acoustic beam [33]. Both effects were observed in experiment [34–36].

Equation (13) can be solved in the case of a parabolic wave front by assuming

$$\psi(x,r,t) = \varphi(x,t) + \frac{r^2}{2}\frac{\partial}{\partial x}\ln f(x,t). \tag{15}$$

With (15), the exact solution of nonlinear equation (13) has the form

$$A = \frac{p_0}{f}\Phi\left(\frac{r}{af}\right)\left[1 + \frac{1}{x_s}\Phi\left(\frac{r}{af}\right)\int_0^x \frac{dx'}{f(x',t)}\right]^{-1}, \tag{16}$$

where p_0 is the initial amplitude on the beam axis and the function Φ describes the initial transverse distribution as $A(x=0,r) = p_0\Phi(r/a_0)$, with a_0 being the initial beam radius. The characteristic nonlinear length

$$x_s = \frac{\pi c^3\rho}{\varepsilon\omega p_0} \tag{17}$$

is the distance at which a break in the wave occurs, and it determines the scale of the nonlinear absorption [31]. If the acoustic nonlinearity is small and the distance x_s is large, the integral term in the square brackets in (16) can be neglected; the function f then describes the changes in both the beam width and the peak pressure on its axis. If the nonlinearity is essential, the shape of the beam changes: because the nonlinear damping is stronger near the axis of the beam, where the peak pressure is large, the initially convex beam becomes flatter and more homogeneous over its cross section.

With (15), eikonal equation (11) becomes

$$\frac{\partial^2 f}{\partial x^2} = f\left(\frac{U_2}{c} + \delta T_2\right), \tag{18}$$

where $T_2(x,t)$ and $U_2(x,t)$ are the coefficients in the transverse-coordinate expansions of the temperature and the flow velocity, respectively:

$$T = T_0 - \frac{r^2}{2}T_2 + \ldots, \qquad U = U_0 - \frac{r^2}{2}U_2 + \ldots.$$

If the temperature and velocity distributions are known, one can find the function f from Eqn (18) and hence solve the problem, i.e., calculate the spatial distribution of the sawtooth wave peak pressure (16) at any time.

In what follows, we assume that self-action occurs in a static medium. The effects associated with the occurrence of flows in sawtooth wave fields and the hydrodynamic convection nonlinearity were discussed in Ref. [37].

The first experiment on thermal self-focusing due to the nonlinear absorption of an ultrasonic wave was described in Ref. [38]. A beam of sawtooth waves at the frequency 2 MHz with the power 20 W and the width 30 mm was transmitted through acetone, which is a weakly absorbing liquid with a negative temperature coefficient of sound velocity, $\delta = -4.6 \times 10^{-3}$ K^{-1}. As a result, a considerable increase in intensity was observed near the beam axis. After 20–30 s, a stationary intensity level was achieved, which was 1.5 times greater than the initial one.

Much later, a series of papers appeared where self-action effects were studied, experimentally and numerically, for sawtooth waves in tissues (see, e.g., Refs [39, 40]). These works were stimulated by practical problems of ultrasonic therapy (hyperthermia) and laser surgery with focused high-intensity acoustic beams. In particular, it turned out that thermal self-action led to a shift of the focal area, which should be taken into account for the accurate focusing of powerful ultrasonic beams on the tissue surface [36].

To describe this effect, we consider the stationary regime in which the time derivative in heat equation (4) is equal to zero. It then follows from (4) that

$$T_2 = \frac{\rho c}{2\varkappa}F = \frac{\varepsilon\omega p_0^3}{3\pi\varkappa c^4\rho^2}\frac{1}{f^3}\left[1 + \frac{1}{x_s}\int_0^x \frac{dx'}{f(x')}\right]^{-3}. \tag{19}$$

Eliminating T_2 from (19) and (18), we obtain the equation for f [41],

$$\left[1 + \Pi\int_0^z \frac{dz'}{f(z')}\right]^3 f^2\frac{d^2 f}{dz^2} = \pm\Pi^3, \tag{20}$$

where Π is the dimensionless amplitude of the wave at the entrance to the medium,

$$\Pi = \frac{x_0}{x_s} = \frac{\pi|\delta|c^2}{3\varkappa\varepsilon\omega}p_0, \qquad x_0 = \frac{\pi^2\delta c^5\rho}{3\varkappa\varepsilon^2\omega^2},$$

and $z = x/x_0$ is the dimensionless longitudinal coordinate. The 'plus' sign on the right-hand side of Eqn (20) corresponds to positive values of the temperature coefficient δ, i.e., to defocusing, and the 'minus' sign corresponds to self-focusing. To obtain the function $f(z)$, one should solve Eqn (20) with the boundary conditions

$$f(z=0) = 1\,, \quad f'(z=0) = K\,,$$

where $K = x_0/R$ is the dimensionless curvature of the wave front at the entrance to the medium.

For the parameters $\Pi = 1$, $K = -1$, nonlinear integrodifferential equation (20) has the exact solution $f = \exp(-z)$. In this special case, as one can see from (16), $A(r=0, z) = p_0$. In other words, the peak pressure on the axis of the initial focused beam is unchanged as a result of the competition between self-defocusing and nonlinear absorption. For other values of the parameters, Eqn (20) should be integrated numerically [41].

Figure 4 shows the dependencies of the beam radius $a(z)$ on the distance. The beam radius is defined as the transverse distance at which the peak pressure is $1/e$ times its value on the beam axis. In the plot, this distance is normalized to the initial beam radius a_0. Solid lines correspond to the case of a defocusing medium ($\Pi = 10$) and dashed lines to a medium without self-action. Thermal defocusing leads to the effects observed in Refs [39, 40]: formation of a finite-sized beam waist and its moving away from the linear focal point. For instance, the lowest curve in Fig. 4 ($K = -100$) can be observed for the following set of parameters: frequency 4 MHz, initial beam radius 3 cm, wave front curvature radius −9.4 cm, and peak pressure 1.3 bar. For such an experiment performed in water or soft tissue, the beam waist moves approximately 1.4 cm from the focal point and its radius is about 3.6 mm, which is an order of magnitude larger than the radius of the diffraction beam waist.

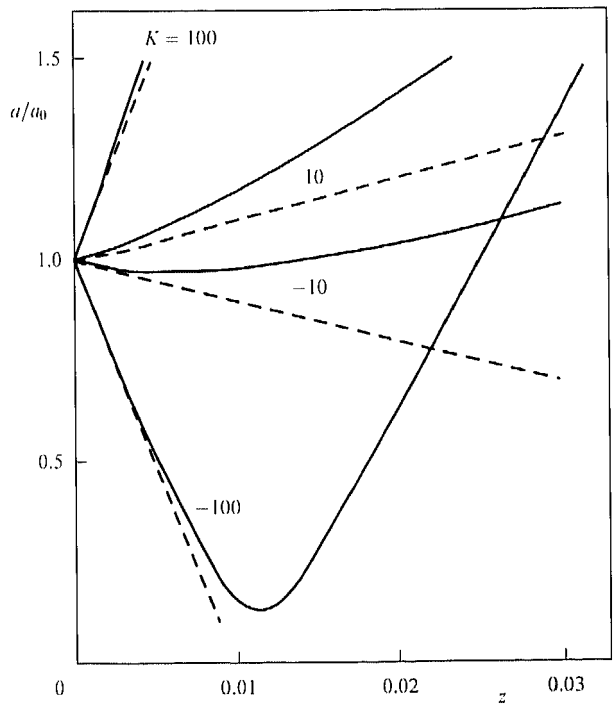

Figure 4. The transverse radius of a sawtooth wave beam plotted versus the distance in the case of thermal self-defocusing. The numbers at the curves indicate the initial dimensionless curvature of the wave front (K). Dashed lines correspond to the absence of thermal self-action.

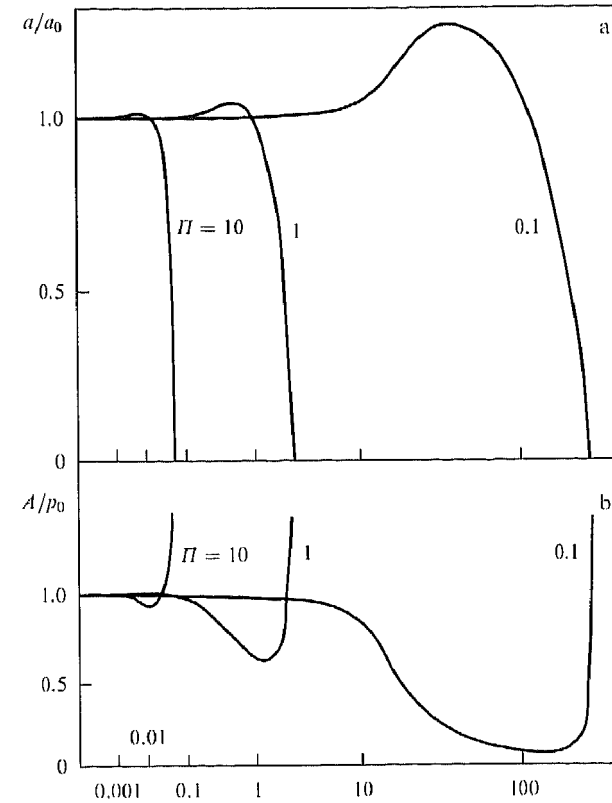

Figure 5. (a) The transverse radius of a sawtooth wave beam as a function of the distance in the case of self-focusing. The numbers at the curves indicate the dimensionless amplitude Π of the wave at the input to the medium. (b) The corresponding dependence for the wave amplitude normalized to its initial value.

Figure 5a shows similar dependences of the beam radius $a(z)/a_0$ on the distance at different values of the dimensionless amplitude $\Pi = 0.1$, 1, 10 for a self-focusing medium. The initial front of the wave is flat. Figure 5b shows the normalized amplitude $A(z)/p_0$ on the beam axis as a function of the distance. For a small Π ($\Pi = 0.1$), the beam radius grows as the wave propagates, i.e., nonlinear broadening of the beam is clearly observed. This effect can be explained by the flattening of the transverse beam profile due to a stronger absorption near the axis (isotropization of the directional distribution). The decrease in the amplitude at small distances is caused by nonlinear absorption, which competes with the self-focusing of the wave front. Near the nonlinear focus, $z = z_f$, inverse dependences are observed: the beam width vanishes and the amplitude becomes infinitely large. In this case, the description becomes inadequate because it does not take the diffraction divergence into account. The distance z_f of self-focusing decreases rapidly with the growth of the amplitude Π.

We now consider the case of nonstationary self-focusing where heat conductivity is small and the diffusion term in Eqn (4) can be neglected. Then,

$$\frac{\partial T}{\partial t} = \frac{c}{c_p} F = \frac{2\varepsilon\omega}{3\pi c^4 \rho^2 c_p} A^3\,. \tag{21}$$

We determine T_2 from (21) by performing the expansion in the transverse coordinate. Substituting the resulting expres-

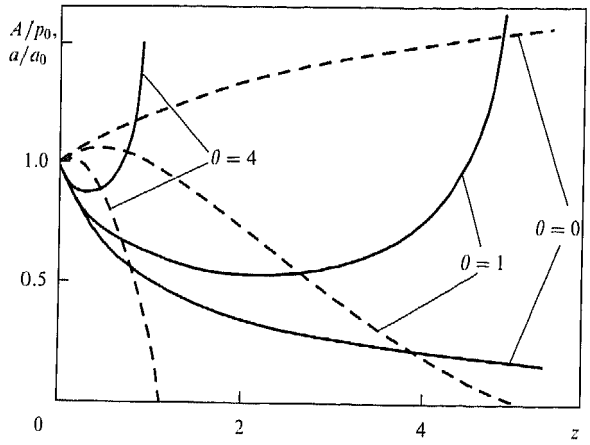

Figure 6. Dependences of the transverse beam radius a/a_0 (dashed curves) and the wave amplitude A/p_0 on the axis (solid curves) on the distance in the case of nonstationary self-focusing. The curves correspond to three consecutive time moments $\theta = 0, 1, 4$.

sion in Eqn (18), for an equation for the function $f(x, t)$ [41],

$$f^5\left[1 + \int_0^z \frac{\mathrm{d}z'}{f(z', \theta)}\right]^4 \frac{\partial}{\partial\theta}\left(\frac{1}{f}\frac{\partial^2 f}{\partial z^2}\right) = \pm 1 . \qquad (22)$$

We introduced here new dimensionless variables

$$z = \frac{x}{x_s}, \quad \theta = \frac{t}{t_0}, \quad t_0 = \frac{\varepsilon\omega\rho c_p a_0^2}{4\pi|\delta|c^2 p_0} . \qquad (23)$$

As before [see (20)], the 'plus' sign on the right-hand side of Eqn (22) corresponds to a positive δ (defocusing) and the 'minus' sign corresponds to self-focusing. The boundary and initial conditions must be chosen as

$$f(z = 0) = f(\theta = 0) = 1 , \quad \frac{\partial f}{\partial z}(z = 0) = \frac{K}{\Pi} = \frac{x_s}{R} . \qquad (24)$$

The problem in (22) and (24) was solved numerically. In Figure 6, the calculated dependences of the beam parameters on the distance are plotted at consecutive time moments θ. The initial front was chosen flat and the medium was assumed to be self-focusing. Dashed lines show the beam radius behavior and solid lines show the corresponding behavior of the amplitude on the axis. One can see that the beam width first grows as z increases and the peak pressure on the axis decreases due to the nonlinear absorption. With time, the thermal lens becomes stronger because the medium is heated up, the beam is focused, and the focal point moves towards the source. The velocity of this motion decreases with time. Similarly to the stationary case, the amplitude of the wave first decreases in the course of propagation, due to the nonlinear absorption, and then, in the vicinity of the focal point, starts to increase rapidly.

3. Self-refraction of weak shock waves in a quadratic nonlinear medium

It was already shown in Ref. [31] that in a dispersion-free quadratic nonlinear medium in the case of small diffraction the transverse distribution of the wave intensity averaged over one period does not change. At the same time, harmonics are generated that have different localizations in space: the higher the harmonic, the narrower its distribution in the near-axis domain. If the beam is broad enough and diffraction is inessential for the fundamental harmonic, it is even less essential for higher harmonics. Hence, the quadratic nonlinearity cannot lead to beam bending or self-focusing. Under such conditions, self-action of a sawtooth wave manifests itself only in the amplitude-dependent absorption. As a result, the central part of the beam is absorbed more than the sides, and the transverse structure of the beam is flattened (isotropized).

In the presence of diffraction, the wave acquires a frequency-dependent phase shift. This leads to the appearance of corresponding phase shifts between the harmonics. Combination of the harmonics with different phases does not give the usual 'saw' profile but instead a more complicated shape [42]: within each period, the compression region becomes higher and sharper and the rarefaction region becomes smoother. The positive pressure peak can even exceed its initial height. Figure 7 demonstrates the signals observed in experiments with intense beams. One can see two periods of the wave, initially harmonic, at some distance from the ultrasound transmitter [43, 35]. Figure 7a shows the oscillogram of a nonlinear acoustic signal in the far-field zone of an unfocused source. Figure 7b shows the profile of the wave in the focal area of a focused source. Theoretical predictions on the nature of the profile distortion are confirmed. Asymmetric profiles similar to the one shown in the figure are typical of intense beams generated by megahertz piezoelectric sources for purposes of medical diagnostics and therapy [43–45].

The fact that the positive peak pressure exceeds the negative one leads to a certain acceleration of the shock front. For instance, in beam focusing, a concave shock front is flattened because of supersonic propagation near the axis as the beam approaches the focus. In other words, self-

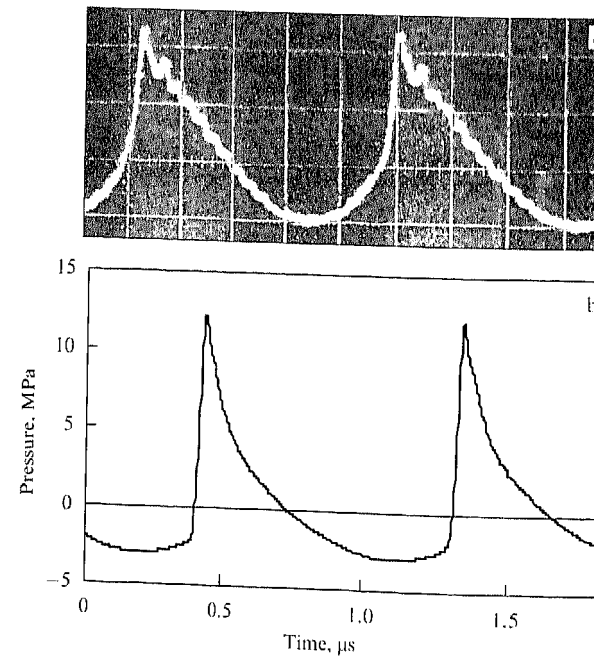

Figure 7. Asymmetric profile distortion for an initially plane wave due to the joint effect of nonlinearity and diffraction: (a) the nonlinear wave profile in the far-field zone of an unfocused ultrasound source [43]; (b) the wave profile in the focal point of an intense focused source [35]. In both cases, the source frequency is 1 MHz.

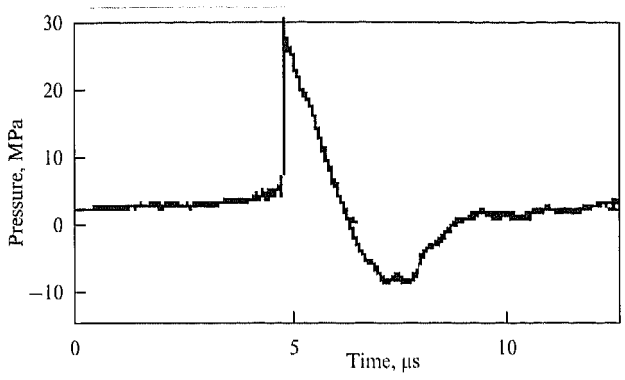

Figure 8. The shape of an acoustic wave registered by a membrane hydrophone in the focus of an electrohydraulic lithotriptor. Usually, the positive-pressure peak precedes the longer tail of negative pressure. Complete destruction of a nephrolith usually requires about 2000 pulses sent at a repetition rate of 1–2 Hz.

defocusing occurs and the peak pressure in the focal area becomes bounded. Another effect reducing the focal intensity is the nonlinear absorption caused by the energy dissipation at shock fronts, especially in the region before the focal point, where diffraction effects are not essential (see also the discussion of pulse self-refraction effects below). However, nonlinear absorption alone cannot prevent the formation of caustics and the occurrence of infinitely large intensities in the course of focusing a sawtooth wave.

In Ref. [46], the possibility of autolocalized propagation of sound beams whose diffraction divergence is compensated by nonlinear instantaneous refraction was considered (similarly to the effect observed in optics [5]). Such localization can possibly be realized over a limited range of wave propagation with the appropriately chosen wave profiles of a special form.

Above, we discussed self-refraction for periodic sawtooth waves. This effect is much more pronounced in the case of single pulses. Self-action of single-pulse signals with shocks [47] is important for a number of applications of nonlinear acoustics and mechanics. Nonlinear pulses can be generated by explosive sources [14], electric discharges [48], or laser radiation [49, 50]. In recent years, field studies of strong pulses have been stimulated by medical applications — shock-wave extracorporal lithotripsy (contact-free noninvasive removal of nephroliths) [50, 51, 36] and remote ultrasonic shear modulus elastometry of soft tissues [52].

In building lithotriptors, the parameters of the focused pulses generated by them were measured. A typical shape of the acoustic pulse in the focal area of an electrohydraulic lithotriptor is shown in Fig. 8. We note that the peak pressure is usually several dozen megapascals and the pulse duration is several microseconds. Investigation of the acoustic fields of lithotriptors revealed several nonlinear phenomena, such as self-refraction, saturation of the peak pressure at the focus, increase in the size of the focal area, shift of the focal area from the ultrasound source, and others [49–51]. The interpretation and mathematical description of these effects has required additional studies.

The self-refraction effect [47] originates from the nonlinear variation of the shock front propagation velocity Δc. This fact is illustrated by Fig. 9, showing the oscillograms of the signal from a broadband hydrophone registering a short intense acoustic pulse in water at various distances from the acoustooptic source [53]. The signal has a steadily triangular shape with a shock front. As the distance increases, the peak pressure is reduced and the pulse width grows. The origin of the time scale in the consecutive oscillograms is chosen in accordance with the delay calculated from the known velocity of weak acoustic perturbations (the speed of sound). With this choice of the initial delay, weak signals registered at various distances are in the same part of the oscillogram. One can see that in contrast to weak signals, the shock front seen in the oscillogram is shifted to the left, i.e., propagates faster than waves of infinitely small amplitude.

For pulses propagating in an unperturbed medium, the nonlinear component Δc of the shock front velocity grows with the increase in the pressure step A as $\Delta c = \varepsilon A/2c\rho$. Because the value of A on the beam axis is larger than in remote regions, the flattening of the focused wave front is observed. Self-refraction is often accompanied by the formation of so-called shock-shocks [4], i.e., breaks in the shock fronts. The structure of the shock front in this case resembles the front structure observed for the 'Mach' reflection of a shock wave from a solid surface [54, 55]. Nonlinear absorption, which occurs simultaneously with self-refraction, makes the distribution of A over the front more uniform. This effect decelerates the self-refraction and results in an almost flat wave front in the paraxial area near the focus. Evidently, both processes should shift the nonlinear focus with respect to the geometric one and increase the beam waist. These effects were observed in the experiments described in review [13].

Nonlinear behavior of a single focused pulse was described in Ref. [56] using the standard Khokhlov–Zabolotskaya equation [Eqn (1) with $U_x = T = b = 0$]. After the change of variables in (9), in the approximation of nonlinear geometric acoustics, we obtain the two equations

$$\frac{\partial p}{\partial x} - \frac{\varepsilon}{c^3\rho}\left(p - \frac{A}{2}\right)\frac{\partial p}{\partial \theta} + \frac{\partial p}{\partial r}\frac{\partial \psi}{\partial r} + \frac{p}{2}\Delta_\perp \psi = 0\,, \tag{25}$$

$$\frac{\partial \psi}{\partial x} + \frac{1}{2}\left(\frac{\partial \psi}{\partial r}\right)^2 = -\frac{\varepsilon}{2c^2\rho}A \tag{26}$$

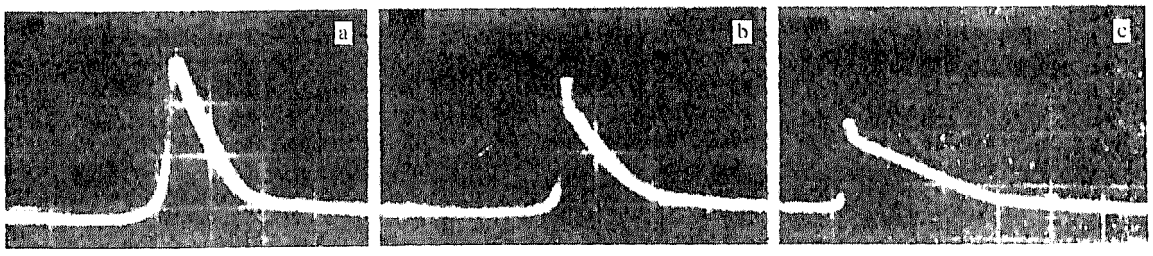

Figure 9. The profile of an intense acoustic pulse in water at various distances from the optoacoustic source: $x = 0$ (a), 4 cm (b), and 8 cm (c). The vertical scale is 4 MPa per division, the horizontal scale is 200 ns per division.

in the region where the shock front has a peak pressure A. A similar system with $A = 0$ describes the pulse at the stage before its shock front is formed.

Assuming that the front is parabolic [see Eqn (15)] and changing the variables as

$$P = f(x)\,p\,, \quad B = f(x)A\,, \quad \zeta = \frac{r}{af}\,, \quad \xi = \int_0^x \frac{\mathrm{d}x'}{f(x')}\,, \tag{27}$$

we reduce the transport equation to the equation of a simple-wave type,

$$\frac{\partial P}{\partial \xi} - \frac{\varepsilon}{c^3\rho}\left(P - \frac{B}{2}\right)\frac{\partial P}{\partial \theta} = 0\,, \tag{28}$$

which can be easily solved. As a result, we obtain the peak pressure in a single pulse that initially has the shape of an isosceles triangle with the duration $2T_0$:

$$A(x, r) = \frac{p_0}{f}\,\Phi\left(\frac{r}{af}\right)\left[1 + \frac{1}{2x_s}\,\Phi\left(\frac{r}{af}\right)\int_{x_1}^{x}\frac{\mathrm{d}x'}{f(x', t)}\right]^{-1/2}. \tag{29}$$

Here, $x_1 = R[1 - \exp(-x_s/R)]$ is the distance at which a break is formed in the focused wave and $x_s = c^3\rho T_0/\varepsilon p_0$ is the distance at which a break is formed in the corresponding plane wave. Substituting (29) in eikonal equation (26), we obtain [57]

$$f^2\frac{\mathrm{d}^2 f}{\mathrm{d}x^2} = \frac{1}{2x_s x_d}\left[1 + \frac{1}{4x_s}\int_{x_1}^{x}\frac{\mathrm{d}x'}{f(x', t)}\right] \times \left[1 + \frac{1}{2x_s}\int_{x_1}^{x}\frac{\mathrm{d}x'}{f(x', t)}\right]^{-3/2}, \tag{30}$$

where $x_d = a^2/2cT_0$ is the typical diffraction scale. The boundary conditions at $x = x_1$ are

$$f = 1 - \frac{x_1}{R}\,, \quad \frac{\mathrm{d}f}{\mathrm{d}x} = -\frac{1}{R}\,. \tag{31}$$

The solution of the problem in (30) and (31) depends on two dimensionless parameters, which can be chosen as $\Pi = R/x_s$ (dimensionless peak pressure) and $D = R/x_d$ (dimensionless diffraction beam waist).

Equation (30) with boundary conditions (31) was solved numerically in Ref. [56]. A typical nonlinear dependence of the pressure on the distance has four different sections (Fig. 10). At first, the peak pressure grows due to wave focusing (section ab). Then, after the break, nonlinear absorption starts to dominate and, despite the focusing, the peak pressure can even decrease (section bc). The pressure grows in approaching the focus (section cf) and reaches its maximum at some point $x > R$. Finally, in the fourth section, behind the focus (section fd), the pressure decreases due to both geometric divergence and nonlinear absorption.

An important feature is a decrease in the maximal peak pressure A_{max} with the growth of p_0. At small values of Π, the maximum of the peak pressure is achieved at the focus, $x = R$, and reaches a large value of p_0/D [57]. At sufficiently large initial values (for instance, at $\Pi \geqslant 100$ for $D = 0.01$, see Fig. 10), there is no amplification at all. It is important to note that the nonlinear decrease in the pulse amplitude also occurs in the absence of self-refraction, because the wave is nonlinearly absorbed due to the energy dissipation at the shock front. But this mechanism is unable to limit the peak

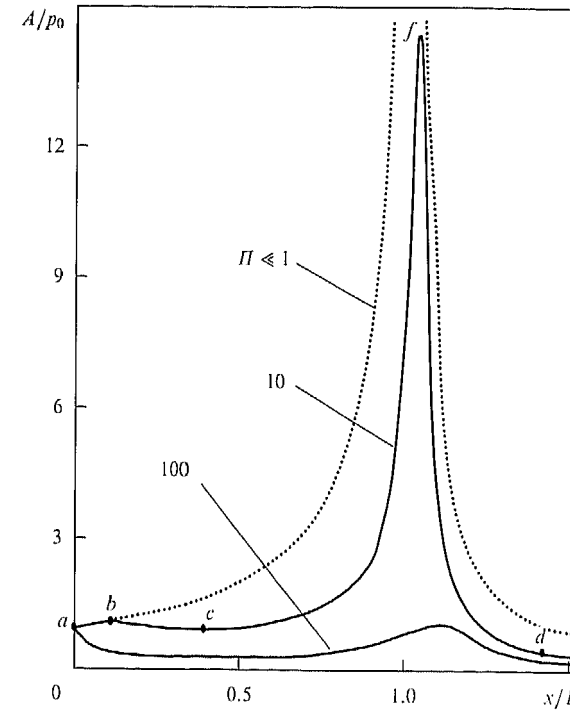

Figure 10. Peak pressure A on the beam axis of an acoustic pulse normalized to its initial value p_0 and plotted versus the dimensionless distance x/R at $D = 0.01$. Solid curves show the dependences for the pulse dimensionless amplitudes $\Pi = 10$ and 100, the dashed curve shows the result of the linear theory ($\Pi \ll 1$).

pressure of a pulse at some distance from the source, unlike in the case of periodic sawtooth signals. For instance, in the case of one-dimensional propagation, the peak pressure in an acoustic pulse at a fixed distance has a square-root dependence on the initial peak pressure, $A_{max} \sim \sqrt{p_0}$ [31]. Self-refraction (self-defocusing) additionally reduces the maximal peak pressure. To demonstrate this effect, a detailed numerical study of the problem in (29)–(31) was carried out. With a high accuracy, the calculated value of the nonlinear 'amplification coefficient' A_{max}/p_0 for a broad range of Π and D variation turned out to be inversely proportional to the product ΠD. This fact led to the important conclusion that the maximum possible peak pressure A_{max} is independent of the initial wave amplitude p_0.

Therefore, refraction leads to the new phenomenon of 'nonlinear saturation' — bounding the peak pressure in focused pulses. According to calculations [56],

$$A_{max} \sim 1.5 p_* \alpha^2\,, \tag{32}$$

where $p_* = \rho c^2/2\varepsilon$ is the typical internal pressure in the liquid and $\alpha = a_0/R$ is the tangent of half the convergence angle for the initial focused beam. It follows from empirical formula (32) that the maximal possible pressure in the focus is approximately equal to the product of the typical internal pressure in the medium and the squared half convergence angle for the initial beam. For a beam with the convergence angle 30° in water ($p_* = 320$ MPa), estimate (32) gives $A_{max} = 130$ MPa, which is in agreement with the experimental data [51].

Thus, nonlinearity has a strong effect on the focusing of pulsed signals. In addition to absorption at shock fronts, nonlinearity leads to self-focusing due to the dependence of

the front velocity on the peak pressure. Because of this effect, the size of the focal spot can greatly exceed its value in the absence of nonlinearity; moreover, it grows with the increase in the initial 'amplitude'. The longitudinal size of the focal area also increases, i.e., nonlinear effects on the whole 'smear' the beam waist. In addition, the transverse distribution of the 'amplitude' becomes more uniform, and the nonlinear focus is formed at distances greater than the linear one. The 'amplitude' of the pulse at the focus is practically independent of p_0 at sufficiently large values of p_0, i.e., nonlinear saturation takes place.

4. Instantaneous self-action in a cubic nonlinear medium

In most cases, the nonlinear response of a medium is delayed in time. An example is the thermal self-action described above, with the nonlinear response being caused by the inertial process of heating. Sometimes, however, the opposite situation occurs, where the nonlinear response is almost instantaneous, i.e., its time delay is much smaller than the wave period or the pulse duration. In nonlinear optics, all basic instantaneous self-action effects are related to the cubic nonlinearity that manifests itself in the background of strong dispersion. It is therefore interesting to also find the role of the cubic nonlinearity under the condition of weak dispersion. It can be shown that propagation of dispersionless wave beams in a medium with a cubic nonlinearity is described by the equation

$$\frac{\partial}{\partial\tau}\left[\frac{\partial p}{\partial x}+\gamma p^2\frac{\partial p}{\partial\tau}-\beta\frac{\partial^2 p}{\partial\tau^2}\right]=\frac{c}{2}\Delta_\perp p\,, \tag{33}$$

where, as in Eqn (1), the respective coefficients β and γ characterize the dissipative and nonlinear properties of the medium, the function $p(x,y,z,\tau=t-x/c)$ describes the wave profile, x is the coordinate along the beam propagation direction, and y and z are the transverse coordinates of the beam [58–60].

An example of a cubic nonlinear effect in acoustics is the formation of shear waves in a defect-free solid. In this case, the role of the function p in (33) is played by the shear stress or the vibrational velocity of particles in the medium. Shear waves can exist not only in classical solids but also in gel-type materials like rubbers or tissues. In such media, the shear modulus is small compared to the compression modulus; as a result, large shear deformations are easily available, which gives rise to considerable values of the elastic nonlinear response. Although shear waves in tissue usually have strong absorption, nonlinear effects can essentially manifest themselves before the wave is absorbed. Shear waves in tissues are interesting because they can be used in the diagnostics of tumor-like masses. As a rule, a diseased tissue has a much higher shear modulus than a healthy one. (This fact has been known for a long time and underlies the traditional palpation method.) Shear waves are most efficiently excited in the bulk of tissue by means of the radiation force caused by the absorption of longitudinal ultrasonic wave beams [61, 52]. This source of shear waves can be made more efficient by using focused ultrasound with a sawtooth wave profile, whose radiation pressure on the medium is increased due to the effect of nonlinear absorption [35]. Another way of generating high-amplitude shear waves in the bulk of a tissue is to use a source moving with a 'near-sonic' velocity, i.e., with the velocity of the shear waves it generates. The theory of such excitation of nonlinear waves was considered in Refs [62, 63]. If the source moves with a 'supersonic' velocity, the waves are generated most efficiently along the corresponding Mach cone. The velocity of shear waves in tissues is comparatively small, about several meters per second. Therefore, a near-sonic or supersonic source can be created by scanning the exciting ultrasound beam in space. This possibility was recently demonstrated in experiments reviewed in Ref. [64].

Instantaneous self-action based on the model in (33) was studied in Refs [58, 60, 65–68]. The usual approach to the description of dispersive media consists of passing from field equation (33), by means of (6), to a Schrödinger-type equation for the complex amplitude

$$\frac{\partial A}{\partial x}+\beta\omega^2 A=\frac{\mathrm{i}}{2k}\Delta_\perp A+\mathrm{i}\gamma\omega|A|^2 A\,, \tag{34}$$

where $k=\omega/c$. In the dispersionless case, this approach is not valid for the following reasons.

On the one hand, it was shown in Ref. [7] that Eqn (34) with $\beta=0$ describes the instability of a flat wave front in the cases where the wave intensity exceeds the critical value:

$$A^2>A_{\mathrm{cr}}^2=\frac{c}{\gamma\omega^2}\,\frac{a_1^2+a_2^2}{a_1^2 a_2^2}\,. \tag{35}$$

The amplitude of each spatial harmonic of the perturbation $A'(x)\cos(y/a_1)\cos(z/a_2)$ then grows exponentially with an increase in the distance (y,z are transverse coordinates of the beam). Thus, a plane wave in a self-focusing medium under condition (35) is unstable: it splits into separate self-focusing beams whose power is approximately equal to the critical one.

On the other hand, Eqn (34) is derived under the assumption that the wave profile is harmonic. But due to the absence of dispersion, the wave that is initially plane and harmonic is distorted according to Eqn (33) and transforms into a sawtooth signal [69, 58]. In a cubic nonlinear medium, in contrast to quadratically nonlinear media [31], the 'saw teeth' are trapezoid-shaped (Fig. 11). Because of nonlinear absorption at shock fronts, the perturbation 'amplitude'

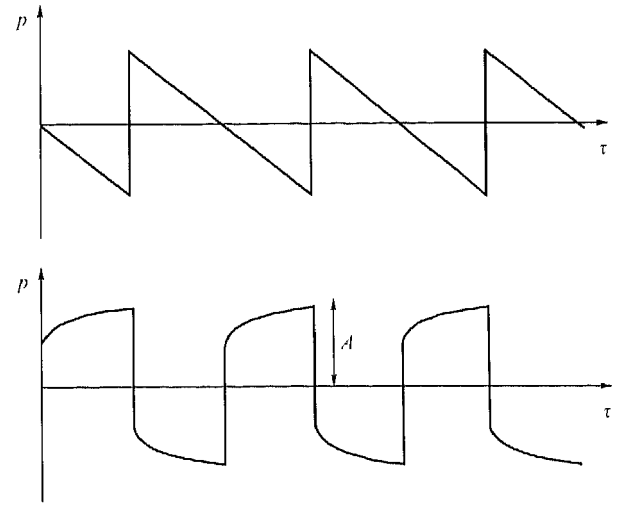

Figure 11. The profile of a sawtooth wave in a medium with a cubic nonlinearity (below) differs from the one with a quadratic nonlinearity (above).

decreases as

$$A(x) = A_0(1 + \alpha\gamma\omega A_0^2 x)^{-1/2},$$

where $\alpha = (3 - 2\ln 2)/4\pi = 0.1284\ldots$.

Thus, the nonlinear term $\gamma p^2 \partial p/\partial\tau$ in Eqn (33) is responsible for two opposite processes, the growth of the amplitude due to self-focusing and the nonlinear absorption due to the formation of shock fronts. Clearly, Eqn (34) is not applicable to dispersionless waves because nonlinear dispersion is masked by strong nonlinear absorption. The significance of nonlinear absorption can be illustrated by the behavior of a plane sawtooth wave. Nonlinear dispersion for such a wave manifests itself in the amplitude-dependent growth of the wave propagation velocity. It can be shown that in the course of propagation, the time shift $\Delta\tau$ of the wave profile depends on the distance according to the logarithmic law [58]

$$\omega\Delta\tau = \frac{1}{4\alpha}\ln(1 + \alpha\gamma\omega A_0^2 x).$$

Clearly, the nonlinear dispersion becomes weaker at large distances as the wave amplitude decreases due to the nonlinear absorption. Using the known law of the amplitude decay (see above), we can find the relation between the wave amplitude and the corresponding nonlinear phase shift:

$$A(x) = A_0 \exp(-2\alpha\omega\Delta\tau).$$

At a distance where the nonlinear phase shift is equal to 2π (one-wave phase shift), the amplitude is noticeably reduced: $A \approx 0.2A_0$, and a three-wave phase shift already corresponds to a negligibly small amplitude, $A \approx 0.008A_0$. Therefore, although diffraction can change the type of self-action in a wave beam, our estimates of nonlinear absorption indicate that an adequate description of self-focusing requires approaches that account for the specific features of sawtooth waves, in particular, their considerable absorption.

Using (9) and passing to the approximation of nonlinear geometric acoustics, we obtain two equations instead of (33): the transport equation

$$\frac{\partial p}{\partial x} + \gamma(p^2 - \langle p^2\rangle)\frac{\partial p}{\partial\theta} - \beta\frac{\partial^2 p}{\partial\theta^2} + \nabla_\perp\psi\,\nabla_\perp p + \frac{p}{2}\Delta_\perp\psi = 0 \tag{36}$$

and the eikonal equation

$$\frac{\partial\psi}{\partial x} + \frac{1}{2}(\nabla_\perp\psi)^2 = \gamma c\langle p^2\rangle. \tag{37}$$

We next multiply (36) by p and take the time average over the period. As a result, we obtain an equation for the average intensity,

$$\frac{\partial I}{\partial x} + \nabla_\perp\psi\,\nabla_\perp I + I\Delta_\perp\psi = -2\beta\left\langle\left(\frac{\partial p}{\partial\theta}\right)^2\right\rangle, \qquad I = \langle p^2\rangle. \tag{38}$$

The right-hand side of Eqn (38) is related to the nonlinear energy dissipation at shock fronts. It can be calculated from expressions describing the structure of the fronts. In a periodic trapezoidal 'saw', a compression shock wave has the form of a step between the values $-A$ and $A/2$ and a rarefaction shock wave between A and $-A/2$ [69]. The compression region in the period with a number n is implicitly described by the relation

$$\ln\left|\frac{1 + 2p/A}{1 - p/A}\right| + \frac{3}{1 - p/A} = \frac{9\gamma}{2\beta}A^2(\theta - \theta_n). \tag{39}$$

A similar formula is valid for negative half-periods (rarefaction regions). Calculating the right-hand side of (38) from (39) and assuming the nonlinear dissipation to be infinitely small, we obtain the system of equations [58]

$$\frac{\partial I}{\partial x} + \frac{\partial}{\partial r}(IV) + \frac{m}{r}IV = -\alpha\omega\gamma I^2, \tag{40}$$

$$\frac{\partial V}{\partial x} + V\frac{\partial V}{\partial r} = \gamma c\frac{\partial I}{\partial r}, \tag{41}$$

where $m = 0$ for a planar (slit) beam and $m = 1$ for an axially symmetric round beam, and $V = \partial\psi/\partial r$ is the angle between a given acoustic ray and the beam axis. The coefficient $\alpha \approx 0.13$ is determined by the profile structure of the trapezoidal 'saw'. System (40), (41) resembles the equations for the flow of a barotropic incompressible liquid, which have previously been applied to the analysis of aberrational self-focusing of light [1]. The principal distinguishing feature of system (40), (41) is that it involves the nonlinearity $\sim\gamma$ in both equations. The right-hand side of Eqn (40) is then responsible for nonlinear absorption and the right-hand side of Eqn (41) for beam bending. In the optical case, the nonlinear absorption is absent and the corresponding system can be exactly solved for $m = 0$.

In our case, system (40), (41) also has interesting solutions. For parabolic front (15), the exact solution of (40) at $m = 1$ is

$$I = \frac{1}{f^2(x)}I_0\left(\frac{r}{af}\right)\left[1 + \alpha\omega\gamma I_0\left(\frac{r}{af}\right)\int_0^x\frac{\mathrm{d}x'}{f^2(x')}\right]^{-1}, \tag{42}$$

where the function $I_0 = I_0(r/a) = \langle p^2\rangle|_{x=0}$ gives the transverse distribution of the wave intensity at the entrance to the medium, a is the typical transverse size (radius) of the initial beam, and the function $f(x)$ describes the variation in the wave amplitude and the beam width. With (42), Eqn (41) can be reduced to a nonlinear integrodifferential equation for f,

$$f^3\frac{\mathrm{d}^2 f}{\mathrm{d}x^2} = -\frac{1}{2x_\mathrm{d}x_\mathrm{s}}\left[1 + \frac{\alpha}{x_\mathrm{s}}\int_0^x\frac{\mathrm{d}x'}{f^2(x')}\right]^{-2}, \tag{43}$$

where the typical distance x_s at which the break occurs and the diffraction length x_d are given by combinations of the constants, $x_\mathrm{s} = 1/(\omega\gamma p_0^2)$, $x_\mathrm{d} = \omega a^2/2c$, and p_0 and ω are the typical initial amplitude and frequency, respectively. Equation (43) must be solved with the boundary conditions

$$f\Big|_{x=0} = 1, \qquad \frac{\mathrm{d}f}{\mathrm{d}x}\Big|_{x=0} = \frac{1}{R}, \tag{44}$$

where R is the curvature radius of the wave front at the input of the medium. The Cauchy problem in (43) and (44) has the exact solution [58]

$$f(x) = \left(1 + \frac{x}{R} + \delta_1\frac{x}{x_\mathrm{s}}\right)^{\delta_2/(\delta_1+\delta_2)}\left(1 + \frac{x}{R} - \delta_2\frac{x}{x_\mathrm{s}}\right)^{\delta_1/(\delta_1+\delta_2)}, \tag{45}$$

where

$$\delta_{1,2} = \frac{\sqrt{\alpha^2 + 2x_s/x_d} \pm \alpha}{2}.$$

It follows that if we neglect the diffraction, we obtain a beam converging to a point at the distance $x_{sf} = (\delta_2/x_s - 1/R)^{-1}$. Clearly, the diffraction cannot be neglected at this stage. The divergence at the focus can be eliminated by adding the diffraction correction [58, 68]

$$f^3 \frac{d^2 f}{dx^2} = -\frac{1}{2x_d x_s}\left[1 + \frac{\alpha}{x_s}\int_0^x \frac{dx'}{f^2(x')}\right]^{-2} + \frac{1}{x_d^2} \qquad (46)$$

to the right-hand side of (46). Surprisingly, even in this case, there exists an exact analytic solution. It can be found by passing to a new variable in Eqn (46),

$$\xi = \frac{x_s}{\alpha x_d} + \frac{1}{x_d}\int_0^x \frac{dx'}{f^2(x')}. \qquad (47)$$

With (47), Eqn (46) becomes linearized:

$$\frac{d^2}{d\xi^2}\left(\frac{1}{f}\right) + \left(1 - \frac{x_s}{\alpha^2 x_d}\frac{1}{\xi^2}\right)\left(\frac{1}{f}\right) = 0. \qquad (48)$$

The general solution of (48) is expressed in terms of the Bessel functions:

$$f(\xi) = \frac{\xi^{-1/2}}{C_1 J_\nu(\xi) + C_2 Y_\nu(\xi)}, \qquad \nu = \frac{1}{2}\sqrt{1 + \frac{2x_s}{\alpha^2 x_d}}. \qquad (49)$$

The constants C_1 and C_2 in (49) can be determined from boundary conditions (44) at $x = 0$, i.e., at $\xi = x_s/\alpha x_d$: $f = 1$, $df/d\xi = x_d/R$. This exact solution was analyzed in detail in Ref. [68]: the minimal beam width and the angular divergence in the far-field zone were calculated, and the dependences of the beam width and the wave amplitude on the distance were found.

Figure 12 shows the dependence of the beam width on the distance normalized to the value that gives the position of the nonlinear focus in the absence of diffraction, $x_{sf} = x_s/\delta_2$. The input front is flat. Curves *1–4*, in ascending order, correspond to decreasing values of the wave amplitude. One can see that at weak diffraction, the beam is noticeably narrowed (curves *1* and *2*), and at strong diffraction there is no self-focusing (curves *3* and *4*).

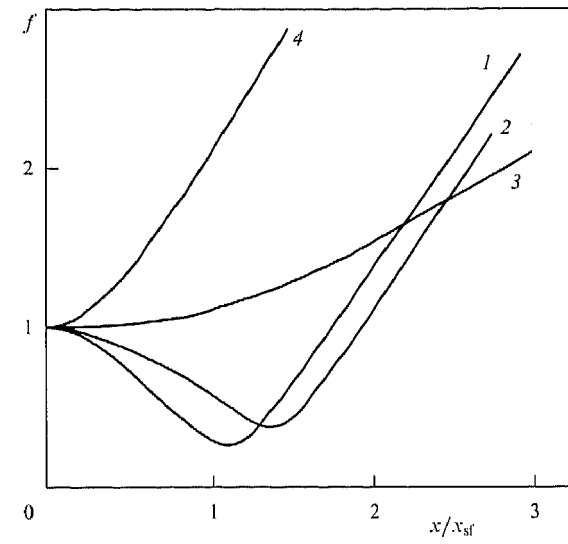

Figure 12. The function f giving the dimensionless transverse radius of the beam versus the dimensionless distance along the axis x/x_{sf}. Curves *1–4* were calculated for different relations between the diffraction and nonlinear lengths: $x_s/x_d = 0.01, 0.1, 0.5$, and 2, respectively.

Figure 13 shows the behavior of the function f describing the beam width in the absence of diffraction (dashed curves *1*). The curves were plotted using Eqn (45). Solid curves *2* (for f) and *3* (for the 'saw amplitude' A) were plotted with diffraction corrections taken into account, i.e., based on the solution of Eqn (46). One can see that at small distances the amplitude decreases because of the nonlinear energy dissipation at the shock fronts of the sawtooth wave. Further, nonlinear focusing 'slows this process down' and can even increase the wave intensity in the focal area. Behind the focus, the beam becomes divergent, and the wave amplitude decreases due to the divergence and nonlinear absorption. Figures 13a–c are plotted in descending order for the initial wave amplitude, i.e., for the parameter x_s/x_d being 10^{-3}, 10^{-2}, and 10^{-1}, respectively.

As follows from Fig. 13, self-focusing due to the cubic nonlinearity does not lead to a considerable growth in the

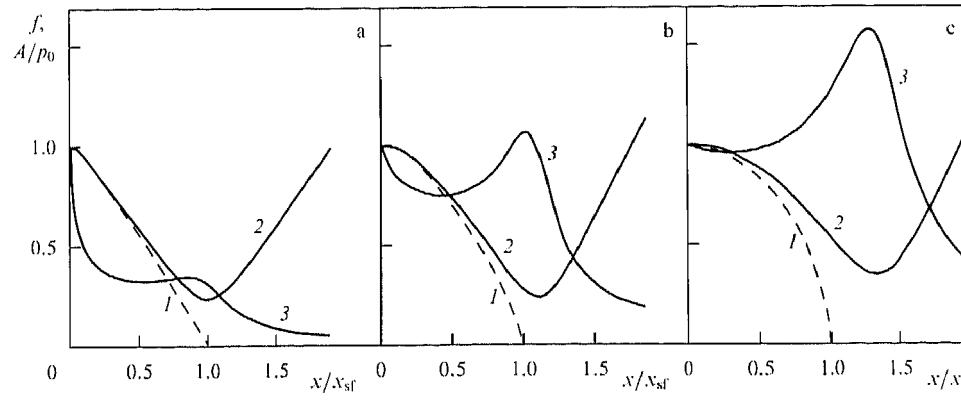

Figure 13. Dependences of the beam parameters on the distance along the axis for the self-focusing of a sawtooth wave in a cubic nonlinear medium in the absence of dispersion. Figures a, b, c correspond to different ratios of the nonlinear and diffraction lengths: $x_s/x_d = 10^{-3}, 10^{-2}$, and 10^{-1}. Dashed lines *1* show the dimensionless transverse radius of the beam in the absence of diffraction, curves *2* show the same value with diffraction taken into account, and curves *3* correspond to the wave amplitude A normalized to its initial value p_0.

amplitude in the absence of dispersion. Although the beam becomes noticeably narrower and a nonlinear beam waist appears, amplification is weak because of the inevitable absorption at the shock fronts of the 'saw'. The largest amplification at the focus is ~ 1.65 and can be achieved at $x_s/x_d \approx 0.06$ [58]. Thus, self-focusing does not lead to a strong intensity growth for sawtooth waves: the absence of dispersion 'switches off' one of the most outstanding nonlinear effects typical of optical beams.

5. Symmetries and conservation laws for the parabolic equation describing propagation of beams in a nonlinear medium

From the above consideration, we see that nonlinear parabolic equations like (1) and (33) describe a broad variety of phenomena observed for wave beams in media with various types of nonlinearities. It is interesting to study the general properties of the solutions of these equations, such as symmetries and conservation laws. We consider the generalized nonlinear parabolic equation

$$\frac{\partial}{\partial\tau}\left[\frac{\partial u}{\partial x}+P(u)\,\frac{\partial u}{\partial\tau}\right]=\frac{\partial^2 u}{\partial y^2}+\frac{\partial^2 u}{\partial z^2}\,, \tag{50}$$

where the function u determines the wave profile, τ is the 'running' time, x is the coordinate along the beam, and y and z are the transverse coordinates. In the absence of diffraction, Eqn (50) turns into the Riemann equation

$$\frac{\partial u}{\partial x}+P\,\frac{\partial u}{\partial\tau}=0\,,$$

i.e., $P(u)$ characterizes the nonlinear component of the wave velocity. Equation (50) is a generalization of the Khokhlov–Zabolotskaya (KZ) equation in the case of media with an arbitrary nonlinearity. It can be shown that (50) is the quasi-optical approximation of the nonlinear wave equation

$$\Delta u-\frac{1}{c^2}\,\frac{\partial^2 u}{\partial t^2}=\frac{\partial^2 N(u)}{\partial t^2}\,,$$

where the right-hand side can be alternatively given by a mixed space–time derivative or the second spatial derivative of the nonlinear function $N(u)$. The function P in Eqn (50) is proportional to the derivative of N with respect to its argument. This relation between the generalized KZ equation and the nonlinear wave equation implies that Eqn (50) can describe beams of various origins. For sound beams in liquids and gases, u is the vibrational velocity or acoustic pressure and the nonlinearity is quadratic: $P(u)=u$. In the case of the cubic nonlinearity described above, $P(u)=u^2$.

Equation (50) takes into account two effects that determine the behavior of wave beams: nonlinearity and diffraction. But it ignores the energy dissipation of the wave, which is of considerable importance in highly viscous media and has a certain influence on the after-shock regions of waves in weakly viscous media. Equation (50) provides a correct description of a nonlinear beam before the formation of a shock. To take dissipation into account, an additional term should be introduced into the square brackets on the left-hand side of (50). This term is proportional to $\partial^2 u/\partial\tau^2$ [see Eqn (58), as well as Eqns (1) and (33)].

Because (1) is a nonlinear equation, it can be solved only numerically in the general case. However, this calculation requires a large amount of computer time and is not always possible. It is therefore important to find alternative approaches to the analysis of the KZ equation. In addition to various approximate methods (one of which was used above), it is interesting to consider the symmetries of this equation. Symmetry properties of a nonlinear equation allow us to find some general features of its solutions, discover certain classes of solutions, and formulate conservation laws. As an example of the symmetry approach, we mention the well-known theory of similarity and dimensionality, which is based on the invariance of some equations under an appropriate stretching of the function and its coordinates. The symmetry class of a differential equation is often wider than the similarity considerations would predict. The symmetry class can be found by means of a technique based on the group-theoretical analysis of differential equations [70–73]. The symmetry of the KZ equation was first studied in Ref. [74], where a two-dimensional equation with a quadratic nonlinearity was considered [$\partial/\partial y=0$, $P(u)=u$]. Another approach, in which a relation was found between a limiting case of the two-dimensional KZ and the Kadomtsev–Petviashvili equation, was considered in Ref. [75]. The results of the group-theoretical analysis for the two- and three-dimensional KZ equations with the quadratic nonlinearity $P(u)=u$ can be found in handbook [76]. In Ref. [59], all point (classical) symmetry groups for three-dimensional KZ equation (50) were calculated in the case of an arbitrary smooth function $P(u)$.

Equation (50) can be represented in a slightly different form if in addition to the function u, we use the related function

$$w=\int u\,\mathrm{d}\tau'\,. \tag{51}$$

If u is the vibrational velocity, then w is the displacement of a medium particle. Introducing the notation $w_\mu\equiv\partial w/\partial x_\mu$ and $w_{\mu\nu}=\partial^2 w/\partial x_\mu\partial x_\nu$, we write the resulting equation as

$$w_{01}+P(w_1)w_{11}-w_{22}-w_{33}=0\,. \tag{52}$$

A point symmetry of a differential equation is a set of invertible transformations depending on a continuous parameter λ,

$$\begin{aligned}\tilde{x}_\mu&=X_\mu(x_0,x_1,x_2,x_3,w;\lambda)\,,\\ \tilde{w}&=W(x_0,x_1,x_2,x_3,w;\lambda)\,,\end{aligned} \tag{53}$$

which transform a solution of the equation into another solution of the same equation. In other words, the new function $\tilde{w}$ considered as a function of the new variables $\tilde{x}_\mu$ also satisfies the equation [73]. Usually, the parameter λ is chosen such that at $\lambda=0$, the transformation is the identity. Then, in the first order in λ, we obtain the so-called infinitesimal transformations

$$\begin{aligned}\tilde{x}_\mu&=x_\mu+\lambda\varphi_\mu(x_0,x_1,x_2,x_3,w)\,,\\ \tilde{w}&=w+\lambda\psi(x_0,x_1,x_2,x_3,w)\,,\end{aligned} \tag{54}$$

where the functions φ_μ and ψ give the components of the tangent vector field of the point symmetry group. Using the known φ_μ and ψ, we can restore the corresponding finite

transformations (4) by solving the Lie equations

$$\frac{d\tilde{x}_\mu}{d\lambda} = \varphi_\mu(\tilde{x}_0, \tilde{x}_1, \tilde{x}_2, \tilde{x}_3, \tilde{w}), \qquad \frac{d\tilde{w}}{d\lambda} = \psi(\tilde{x}_0, \tilde{x}_1, \tilde{x}_2, \tilde{x}_3, \tilde{w}) \tag{55}$$

with the initial (at $\lambda = 0$) conditions $\tilde{x}_\mu = x_\mu$, $\tilde{w} = w$.

For Eqn (50), the situation is similar. For instance, infinitesimal transformations of the point symmetry group of Eqn (1) have the form $\tilde{x}_\mu = x_\mu + \lambda\vartheta_\mu(x_0, x_1, x_2, x_3, u)$, $\tilde{u} = u + \lambda\eta(x_0, x_1, x_2, x_3, u)$. Using the group-theoretical analysis [70, 71, 73], one can find the components of the tangent vector field and obtain finite invariant transformations (53). The results of such calculations for all possible point symmetry groups of Eqns (50) and (52) are given in Ref. [59]. The total number of symmetries exceeds twenty. Some symmetries, which correspond to the equation invariance under translations and rotations, turned out to be independent of the form of the nonlinear term. Other symmetries are only possible for certain nonlinearity types. For instance, in the case of a cubic nonlinearity, Eqns (50) and (52) have the symmetry

$$\tilde{u} = u(1 + \lambda x_0), \quad \tilde{w} = w(1 + \lambda x_0), \quad \tilde{x}_0 = \frac{x_0}{1 + \lambda x_0},$$
$$\tilde{x}_1 = x_1 - \frac{\lambda}{4}\frac{x_2^2 + x_3^2}{1 + \lambda x_0}, \quad \tilde{x}_2 = \frac{x_2}{1 + \lambda x_0}, \quad \tilde{x}_3 = \frac{x_3}{1 + \lambda x_0}. \tag{56}$$

From the structure of the invariant transformation one can see that this symmetry can be called a 'lens' transformation. Indeed, a transformation of the same structure was found in Ref. [77] for Eqn (34), which describes the self-action of monochromatic waves in a dispersive medium. The transformation parameter λ then corresponds to the inverse focal length of the lens, i.e., to its 'power'. We note that a similar lens transformation also exists in the linear case. One of its manifestations is the well-known result of the beam theory that the transverse distribution of the wave amplitude in the focal plane of a focused source is identical to the directional diagram of a similar unfocused source in the far-field zone. It is quite unusual that the same property holds for a cubic nonlinear medium, regardless of the wave profile. Analysis of the group properties of two-dimensional (slit) beams has shown that in this case, the lens transformation is invariant only for the fifth-order nonlinearity but not for the third-order one.

In the case of a quadratic nonlinearity, which is also important from the practical standpoint, there is a symmetry that resembles the lens transformation:

$$\tilde{u} = u(1 + \lambda x_0)^{8/5} - \frac{2}{5}\lambda x_1(1 + \lambda x_0)^{3/5} + \frac{3}{50}\frac{\lambda^2(x_2^2 + x_3^2)}{(1 + \lambda x_0)^{2/5}},$$
$$\tilde{w} = w(1 + \lambda x_0)^{6/5} - \frac{1}{5}\lambda x_1^2(1 + \lambda x_0)^{1/5} + \frac{3}{50}\frac{\lambda^2 x_1(x_2^2 + x_3^2)}{(1 + \lambda x_0)^{4/5}} - \frac{3}{500}\frac{\lambda^3(x_2^2 + x_3^2)^2}{(1 + \lambda x_0)^{9/5}},$$
$$\tilde{x}_0 = \frac{x_0}{1 + \lambda x_0}, \quad \tilde{x}_1 = \frac{x_1}{(1 + \lambda x_0)^{2/5}} - \frac{3}{10}\lambda\frac{x_2^2 + x_3^2}{(1 + \lambda x_0)^{7/5}},$$
$$\tilde{x}_2 = \frac{x_2}{(1 + \lambda x_0)^{6/5}}, \quad \tilde{x}_3 = \frac{x_3}{(1 + \lambda x_0)^{6/5}}. \tag{57}$$

The case of quadratic and cubic nonlinearities ($P = u$ and $P = u^2$) with dissipation was studied in Ref. [78], where the group-theoretical analysis was carried out for Eqn (50) with an additional dissipative term,

$$\frac{\partial}{\partial\tau}\left[\frac{\partial u}{\partial x} + P(u)\frac{\partial u}{\partial\tau} + A\frac{\partial^2 u}{\partial\tau^2}\right] = \frac{\partial^2 u}{\partial y^2} + \frac{\partial^2 u}{\partial z^2}. \tag{58}$$

It turned out that the dissipative term breaks some symmetries that exist in the absence of dissipation, in particular, the symmetries given by Eqns (56) and (57). At the same time, accounting for dissipation does not add any new symmetries to Eqn (50). The total number of symmetries for Eqn (58) is eight; one of them is related to a scaling transformation and the others are purely geometric and correspond to translations and rotations.

In addition to the possibility of finding new solutions from the existing ones, equation symmetries have another important application. They can be used for finding the exact solutions and conservation laws of the generalized KZ equation. It is worth noting that Eqn (52) is a Lagrange equation [79]. Indeed, after introducing the specific Lagrangian

$$\Lambda = \frac{w_0 w_1}{2} - \frac{w_2^2 + w_3^2}{2} + F(w_1), \tag{59}$$

where $F(u)$ is obtained by integrating the function $P(u)$ twice, i.e., $d^2F/du^2 = P$, Eqn (52) takes the form

$$\frac{\partial}{\partial x_\mu}\left(\frac{\partial\Lambda}{\partial w_\mu}\right) - \frac{\partial\Lambda}{\partial w} = 0. \tag{60}$$

An equation that can be written in the form of a Lagrange equation is equivalent to a least-action principle [80]. Similarly to the above way of seeking point symmetry groups for Eqn (52), one can search for transformations of form (50) that preserve Lagrange function (59). It was shown in Ref. [60] that all point symmetry groups for Eqn (52), except a single scaling transformation, are variational ones. According to the Noether theorem, each variational symmetry corresponds to a conservation law of the form $D_\mu j_\mu = 0$, where D_μ is the total derivative operator in the coordinate x_μ and j_μ are the components of the 'current'. Hence, it follows that for each variational symmetry, the expression

$$I = \iiint j_0\, dx_1\, dx_2\, dx_3$$

is an integral of motion, i.e., $dI/dx_0 = 0$. Knowing such conservation laws can be useful for the control of numerical simulations and for discovering some basic properties of solutions of the generalized KZ equation. All integrals of motion for Eqn (52) are listed in Ref. [60]. Some of them have a rather clear physical meaning; for instance, one integral of motion is proportional to the Hamiltonian and another one to the total energy of the wave. Other integrals do not permit such clear interpretations but can be used for obtaining some simple relations in terms of the acoustic field moments. The moments are introduced as mean values calculated with the distribution function $u^2 = w_1^2$,

$$\langle F\rangle \equiv \frac{\iiint F w_1^2\, dx_1\, dx_2\, dx_3}{\iiint w_1^2\, dx_1\, dx_2\, dx_3},$$

where F is the variable for which the moment is calculated. For instance, $\langle x_1 \rangle$ gives the position of the time-averaged wave center, $\langle x_{2,3} \rangle$ characterizes the transverse coordinates of the beam cross section center, and $\langle r_\perp^2 \rangle = \langle x_2^2 + x_3^2 \rangle$ is the mean square of the beam cross section radius. In the case of a quadratic nonlinearity, a combination of several integrals gives the relation

$$\frac{\mathrm{d}\langle r_\perp^2 \rangle}{\mathrm{d}x_0} - \frac{4\langle x_1 \rangle}{3} = C_1 + C_2 x_0 ,$$

i.e., the mean-square transverse radius of the beam, $\sqrt{\langle r_\perp^2 \rangle}$, and the position of the acoustic field time-averaged center, $\langle x_1 \rangle$, are related to each other. In the case of a cubic nonlinearity, the behavior of the mean-square radius of the beam is even simpler. Using several variational integrals of motion, one of which follows from lens transformation (56), one can obtain the very important relation

$$\frac{\mathrm{d}^2}{\mathrm{d}x_0^2} \langle r_\perp^2 \rangle = \mathrm{const} = 8 \, \frac{\iiint (w_2^2 + w_3^2 - w_1^4/6) \, \mathrm{d}x_1 \, \mathrm{d}x_2 \, \mathrm{d}x_3}{\iiint w_1^2 \, \mathrm{d}x_1 \, \mathrm{d}x_2 \, \mathrm{d}x_3} , \tag{61}$$

implying that $\langle r_\perp^2 \rangle$ depends on the propagation distance according to a parabolic law. The integral in the numerator of the right-hand side of (61) is the Hamiltonian. If it is negative, then at some finite distance $\langle r_\perp^2 \rangle$ vanishes, i.e., the beam collapses to a point. Thus, the right-hand side of (61) being negative gives a sufficient condition for self-focusing. This condition is very similar to the known Vlasov–Petrishchev–Talanov criterion of wave collapse, which was discovered in 1971 in the framework of nonlinear Schrödinger equation (34) (where $\beta = 0$) and has played an important role in the theory of light beam self-focusing [81]. Later, similar criteria were obtained for a variety of wave models, including the nonlinear Schrödinger equation, the nonlinear Klein–Gordon equation, the nonstationary Ginzburg–Landau equation, the Boussinesq equation, and the generalized Kadomtsev–Petviashvili equation [82]. However, in all these examples, the Hamiltonian is calculated by integrating only over the transverse coordinates, while in our case, the integration also involves the time $\tau = x_1$.

In Ref. [58], the moment $\langle r_\perp^2 \rangle$ was calculated in the case of a Gaussian beam of harmonic waves at the input. It turned out that self-focusing can then only occur if the typical nonlinearity is greater than the diffraction length by almost an order of magnitude. At the same time, the nonlinear focus occurred at a distance greatly exceeding the nonlinear length. Although self-focusing criterion (61) is just a sufficient condition, the estimate in Ref. [58] indicates that self-focusing is hardly possible without the distortion of the wave profile and the formation of shocks. Calculations in the previous section also confirm this feature of self-action in the absence of dispersion.

We point out once again that relation (61) can be written due to the existence of lens transformation (56), which for a three-dimensional beam is only valid for a cubic nonlinearity. For slit beams, a relation of type (61) can be derived for a medium with a fifth-order nonlinearity [79], again due to the existence of an invariant lens transformation in this case. In both cases, that of a three-dimensional beam in a cubic nonlinear medium and that of a two-dimensional slit beam in a fifth-order nonlinear medium, there is no steady-state (self-trapping) solution. Indeed, self-trapping implies the conservation of $\langle r_\perp^2 \rangle$, i.e., the vanishing of the right-hand side of (61). But fluctuations in the initial field may change the right-hand side of (61), leading to a variation of the beam mean-square radius according to (61) and, eventually, to the broadening or collapse of the beam. A question arises: is it possible that steady soliton-like solutions exist for Eqn (50) with other types of nonlinearities, as is the case for wave beams in the presence of strong dispersion? This hardly seems possible because the two effects, nonlinearity and diffraction, should not only ensure stable self-trapping but also prevent nonlinear distortions and shock formation in the wave profile.

6. Conclusion

This review is an extended version of previous publications [83, 84, 33] and covers the most recent developments in the study of self-action effects for strongly distorted waves with shock fronts. Like the previous publications, this review is an attempt to summarize and describe two kinds of self-action phenomena: those already observed for strong acoustic beams and those predicted and, according to the authors' opinion, quite likely to be observed in the nearest future. Many interesting theoretical papers consider new self-action effects that are predicted for strongly distorted waves but whose observation is hardly possible (see, e.g., Ref. [85]). These papers were not discussed in this review and their number in the list of references is small.

One of the basic types of self-action is the thermal one. This effect emerges due to the enhanced heat production in the shock regions. It is inevitable in any nonlinear medium, even if the viscosity is small. The regime of thermal self-defocusing and self-focusing is relevant for strong acoustic waves used in medicine (therapy), where typical intensities of ultrasonic beams can be as high as several thousand Watts per cm^2 and, hence, shock fronts are formed at distances of the order of one centimeter.

Because compression shock waves travel in nonperturbed media with supersonic velocities, another important self-action effect arises — the instantaneous self-refraction of shock-wave pulse beams. This kind of self-action is one of the basic mechanisms limiting the maximal intensity that can be achieved for strong focused pulsed signals.

Still relatively little is known about the self-action of shock waves in weakly dispersive media with a cubic nonlinearity. The nonlinear waves generated under such conditions have unique properties and are quite different from the well-studied nonlinear quasi-harmonic waves in strongly dispersive media. The corresponding equations are complicated and require development of proper analytic and numerical methods; there is still much work to be done in this area.

This work was supported in part by grants by the Russian Foundation for Basic Research and by the program of the President of the Russian Federation for the support of leading scientific schools, grant No. NSh-1575.003.02.

References

1. Akhmanov S A, Sukhorukov A P, Khokhlov R V *Usp. Fiz. Nauk* **93** 19 (1967) [*Sov. Phys. Usp.* **10** 609 (1968)]
2. Vlasov S N, Talanov V I *Samofokusirovka Voln* (Self-focusing of Waves) (Nizhny Novgorod: Izd. IPF RAN, 1997)
3. Karamzin Yu N, Sukhorukov A P *Pis'ma Zh. Eksp. Teor. Fiz.* **20** 734 (1974) [*JETP Lett.* **20** 339 (1974)]

4. Whitham G B *Linear and Nonlinear Waves* (New York: Wiley, 1974) [Translated into Russian (Moscow: Mir, 1977)]
5. Talanov V I *Izv. Vyssh. Uchebn. Zaved. Radiofiz.* **7** 564 (1964) [*Radiophys.* **7** 254 (1964)]
6. Talanov V I *Pis'ma Zh. Eksp. Teor. Fiz.* **2** 218 (1965) [*JETP Lett.* **2** 138 (1965)]
7. Bespalov V I, Talanov V I *Pis'ma Zh. Eksp. Teor. Fiz.* **3** 471 (1966) [*JETP Lett.* **3** 307 (1966)]
8. Fink M *Sci. Am.* **281** (5) 91 (1999)
9. Hynynen K *Sci. Medicine* **3** (5) 1 (1996)
10. Fink M *The e-Journal of Nondestructive Testing* **3** (4) (1998); http://www.ndt.net/article/0498/fink/fink.htm
11. Ing R K, Fink M *Ultrasonics* **36** 179 (1998)
12. Ing R K, Fink M, Casula O *Appl. Phys. Lett.* **68** (2) 161 (1996)
13. Rudenko O V *Usp. Fiz. Nauk.* **165** 1011 (1995) [*Phys. Usp.* **38** 965 (1995)]
14. Lavrent'ev E V, Kuzyan O I *Vzryvy v More* (Explosions in the Sea) (Leningrad: Sudostroenie, 1977)
15. Runyan L J, Kane E J "Sonic boom literature survey", Fed. Av. Admin. Rep. FAA-RD-73-129-II, AD771-274 (1973)
16. Sapozhnikov O A, Khokhlova V A, Cathignol D *J. Acoust. Soc. Am.* **115** 1982 (2004)
17. Zarembo L K, Krasil'nikov V A *Vvedenie v Nelineĭnuyu Akustiku; Zvukovye i Ul'trazvukovye Volny Bol'shoĭ Intensivnosti* (Introduction to Nonlinear Acoustics; Sonic and Ultrasonic High-Intensity Waves) (Moscow: Nauka, 1966)
18. Andreev V G et al. *Akust. Zh.* **45** (1) 13 (1999) [*Acoust. Phys.* **45** 8 (1999)]
19. Askar'yan G A *Pis'ma Zh. Eksp. Teor. Fiz.* **4** (4) 144 (1966) [*JETP Lett.* **4** 78 (1966)]
20. Bakhvalov N S, Zhileĭkin Ya M, Zabolotskaya E A *Nelineĭnaya Teoriya Zvukovykh Puchkov* (Nonlinear Theory of Sound Beams) (Moscow: Nauka, 1982) [Translated into English (New York: American Institute of Physics, 1987)]
21. Assman V A et al. *Pis'ma Zh. Eksp. Teor. Fiz.* **41** 148 (1985) [*JETP Lett.* **41** 182 (1985)]
22. Andreev V G et al. *Pis'ma Zh. Eksp. Teor. Fiz.* **41** 381 (1985) [*JETP Lett.* **41** 466 (1985)]
23. Rudenko O V, Sapozhnikov O A, in *Nonlinear Acoustics* (Eds K A Naugol'nykh, L A Ostrovsky) (New York: AIP Press, 1994) p. 104
24. Bunkin F V, Lyakhov G A, Shipilov K F *Usp. Fiz. Nauk* **165** 1145 (1995) [*Phys. Usp.* **38** 1099 (1995)]
25. Naugol'nykh K A, Ostrovskiĭ L A *Nelineĭnye Volnovye Protsessy v Akustike* (Nonlinear Wave Processes in Acoustics) (Moscow: Nauka, 1990) [Translated into English (New York: Cambridge Univ. Press, 1998)]
26. Vinogradov E A, Shipilov K F *Phys. Vibrations* **10** (2) 72 (2002)
27. Bunkin F V, Kravtsov Yu A, Lyakhov G A *Usp. Fiz. Nauk* **149** 391 (1986) [*Sov. Phys. Usp.* **29** 607 (1986)]
28. Burov A K *Akust. Zh.* **4** (4) 315 (1958)
29. Armeev V Yu, Karabutov A A, Sapozhnikov O A *Akust. Zh.* **33** 177 (1987) [*Sov. Phys. Acoust.* **33** 109 (1987)]
30. Karabutov A A, Rudenko O V, Sapozhnikov O A *Vestn. Mosk. Univ. Ser. 3 Fiz. Astron.* **29** (4) 63 (1988) [*Moscow Univ. Phys. Bull.* **29** (4) 68 (1988)]
31. Rudenko O V, Soluyan S I *Teoreticheskie Osnovy Nelineĭnoĭ Akustiki* (Theoretical Foundations of Nonlinear Acoustics) (Moscow: Nauka, 1975) [Translated into English (New York: Consultants Bureau, 1977)]
32. Novikov B K, Rudenko O V, Timoshenko V I *Nelineĭnaya Gidroakustika* (Nonlinear Hydroacoustics) (Leningrad: Sudostroenie, 1981) [Translated into English (New York: American Institute of Physics, 1987)]
33. Rudenko O V *Izv. Vyssh. Uchebn. Zaved. Radiofiz.* **46** 377 (2003) [*Radiophys. Quantum Electron.* **46** 338 (2003)]
34. Sapozhnikov O A, Sinilo T V *Izv. Ross. Akad. Nauk Ser. Fiz.* **62** 2371 (1998)
35. Pishchal'nikov Yu A, Sapozhnikov O A, Sinilo T V *Akust. Zh.* **48** 253 (2002) [*Acoust. Phys.* **48** 214 (2002)]
36. Bailey M R et al. *Akust. Zh.* **49** 437 (2003) [*Acoust. Phys.* **49** 369 (2003)]
37. Karabutov A A, Rudenko O V, Sapozhnikov O A *Akust. Zh.* **34** 644 (1988) [*Acoust. Phys.* **34** 371 (1988)]
38. Karabutov A A, Rudenko O V, Sapozhnikov O A *Akust. Zh.* **35** 67 (1989) [*Sov. Phys. Acoust.* **35** 40 (1989)]
39. Le Floch C, Tanter M, Fink M *Appl. Phys. Lett.* **74** 3062 (1999)
40. Hallaj I M, Cleveland R O, Hynynen K *J. Acoust. Soc. Am.* **109** 2245 (2001)
41. Rudenko O V, Sagatov M M, Sapozhnikov O A *Zh. Eksp. Teor. Fiz.* **98** 808 (1990) [*Sov. Phys. JETP* **71** 449 (1990)]
42. Rudenko O V, Soluyan S I, Khokhlov R V *Dokl. Akad. Nauk SSSR* **225** 1053 (1975)
43. Andreev V G, Karabutov A A, Rudenko O V *Vestn. Mosk. Univ. Ser. 3 Fiz. Astron.* **25** (4) 74 (1984)
44. Bacon D R *Ultrasound Med. Biol.* **10** 189 (1984)
45. Preston R C (Ed.) *Output Measurements for Medical Ultrasound* (New York: Springer-Verlag, 1991)
46. Makov Yu N *Akust. Zh.* **46** 680 (2000) [*Acoust. Phys.* **46** 596 (2000)]
47. Fridman V E *Akust. Zh.* **28** 551 (1982)
48. Naugol'nykh K A, Roĭ N A *Elektricheskie Razryady v Vode* (Electric Discharges in Water) (Moscow: Nauka, 1971)
49. Askar'yan G A, Korolev M G, Yurkin A V *Pis'ma Zh. Eksp. Teor. Fiz.* **51** 586 (1990) [*JETP Lett.* **51** 667 (1990)]
50. Andreev V G et al. *Akust. Zh.* **38** 588 (1992) [*Sov. Phys. Acoust.* **38** 325 (1992)]
51. Coleman A J, Saunders J E *Ultrasound Med. Biol.* **15** 213 (1989)
52. Sarvazyan A P et al. *Ultrasound Med. Biol.* **24** 1419 (1998)
53. Dubrovskiĭ A N, Sapozhnikov O A *Vestn. Mosk. Univ. Ser. 3 Fiz. Astron.* **34** (4) 67 (1993)
54. Sturtevant B, Kulkarny V A *J. Fluid Mech.* **73** 651 (1976)
55. Higashino F, in *Handbook of Shock Waves* Vol. 2 (Eds G Ben-Dor, O Igra, T Elperin) (San Diego: Academic Press, 2001) p. 397
56. Musatov A G, Rudenko O V, Sapozhnikov O A *Akust. Zh.* **38** 502 (1992) [*Sov. Phys. Acoust.* **38** 274 (1992)]
57. Sapozhnikov O A *Akust. Zh.* **37** 760 (1991) [*Sov. Phys. Acoust.* **37** 395 (1991)]
58. Rudenko O V, Sapozhnikov O A *Zh. Eksp. Teor. Fiz.* **106** 395 (1994) [*JETP* **79** 220 (1994)]
59. Kudryavtsev A G, Sapozhnikov O A *Akust. Zh.* **44** 628 (1998) [*Acoust. Phys.* **44** 541 (1998)]
60. Kudryavtsev A G, Sapozhnikov O A *Akust. Zh.* **44** 808 (1998) [*Acoust. Phys.* **44** 704 (1998)]
61. Andreev V G et al. *Akust. Zh.* **43** 149 (1997) [*Acoust. Phys.* **43** 123 (1997)]
62. Karabutov A A, Rudenko O V *Akust. Zh.* **25** 536 (1979) [*Sov. Phys. Acoust.* **25** 306 (1979)]
63. Karabutov A A, Rudenko O V *Dokl. Akad. Nauk SSSR* **248** (5) (1979)
64. Fink M, in *Book of Abstracts of "Ultrasonics International 2003" Conf., Granada, Spain, June 30 – July 3, 2003*
65. Rudenko O V, in *Advances in Nonlinear Acoustics* (Ed. H Hobæk) (Singapore: World Scientific, 1993) p. 3
66. Rudenko O V, Sapozhnikov O A *Kvantovaya Elektron.* **20** 1028 (1993) [*Quantum Electron.* **23** 896 (1993)]
67. Rudenko O V, Sukhorukov A A *Akust. Zh.* **41** 822 (1995) [*Acoust. Phys.* **41** 725 (1995)]
68. Rudenko O V, Sukhorukov A A *Izv. Ross. Akad. Nauk Ser. Fiz.* **60** (12) 6 (1996)
69. Lee-Bapty I P, Crighton D G *Philos. Trans. R. Soc. London Ser. A* **323** 173 (1987)
70. Ovsyannikov L V *Gruppovoĭ Analiz Differentsial'nykh Uravneniĭ* (Group Analysis of Differential Equations) (Moscow: Nauka, 1978) [Translated into English (New York: Academic Press, 1982)]
71. Ibragimov N Kh *Gruppy Preobrazovaniĭ v Matematicheskoĭ Fizike* (Transformation Groups in Mathematical Physics) (Moscow: Nauka, 1983) [Translated into English: *Transformation Groups Applied to Mathematical Physics* (Dordrecht: D. Reidel, 1985)]
72. Vinogradov A M, Krasil'shchik I S, Lychagin V V *Vvedenie v Geometriyu Lineĭnykh Differentsial'nykh Uravneniĭ* (Introduction to the Geometry of Linear Differential Equations) (Moscow: Nauka, 1986)
73. Olver P J *Applications of Lie Groups to Differential Equations* (New York: Springer-Verlag, 1986) [Translated into Russian (Moscow: Mir, 1989)]

74. Vinogradov A M, Vorob'ev E M *Akust. Zh.* **22** 23 (1976)
75. Kodama Y *Phys. Lett. A* **129** 223 (1988)
76. Ibragimov N H (Ed.) *CRC Handbook of Lie Group Analysis of Differential Equations* Vol. 1 *Symmetries, Exact Solutions, and Conservation Laws*; Vol. 2 *Applications in Engineering and Physical Sciences*; Vol. 3 *New Trends in Theoretical Developments and Computational Methods* (Boca Raton, Florida: CRC Press, 1994–1996)
77. Talanov V I *Pis'ma Zh. Eksp. Teor. Fiz.* **11** 103 (1970) [*JETP Lett.* **11** 64 (1970)]
78. Sapozhnikov O A, Kudryavtsev A G, in *Proc. of the 16th Intern. Congress on Acoustics and 135th Meeting of Acoustical Society of America* Vol. 1 (Eds P K Kuhl, L A Crum) (Woodbury, NY: Acoustical Society of America, 1998) p. 529
79. Makov Yu N, Sapozhnikov O A *Akust. Zh.* **40** 1003 (1994) [*Acoust. Phys.* **40** 889 (1994)]
80. Landau L D, Lifshitz E M *Teoriya Polya* (Field Theory) (Moscow: Nauka, 1988) [Translated into English: *The Classical Field Theory* (Oxford: Pergamon Press, 1975)]
81. Vlasov S N, Petrishchev V A, Talanov V I *Izv. Vyssh. Uchebn. Zaved. Radiofiz.* **14** 1353 (1971) [*Radiophys. Quantum Electron.* **14** 1062 (1971)]
82. Kuznetsov E A *Izv. Vyssh. Uchebn. Zaved. Radiofiz.* **46** 342 (2003) [*Radiophys. Quantum Electron.* **46** 307 (2003)]
83. Rudenko O V, Sapozhnikov O A *Vestn. Mosk. Univ. Ser. 3 Fiz. Astron.* **46** (1) 5 (1991) [*Moscow Univ. Phys. Bull.* **46** 5 (1991)]
84. Rudenko O V, Sapozhnikov O A, in *Nonlinear Acoustics* (Research Trends in Physics, Eds K A Naugol'nykh, L A Ostrovsky) (Woodbury, NY: American Institute of Physics, 1994)
85. Khismatullin D B, Akhatov I Sh *Phys. Fluids* **13** 3582 (2001)